Experimental Brain Research
https://doi.org/10.1007/s00221-022-06513-5

RESEARCH ARTICLE

The motor and the brake of the trailing leg in human walking: transtibial amputation limits ankle–knee torque covariation

Megan E. Toney-Bolger[1,2] · **Young-Hui Chang**[2]

Received: 3 June 2022 / Accepted: 13 November 2022
© The Author(s), under exclusive licence to Springer-Verlag GmbH Germany, part of Springer Nature 2022

Abstract

Lower-limb amputation limits inherent motor abundance in the locomotor system and impairs walking mechanics. Able-bodied walkers vary ankle torque to adjust step-to-step leg force production as measured by resultant ground reaction forces. Simultaneously, knee torque covaries with ankle torque to act as a brake, resulting in consistent peak leg power output measured by external mechanical power generated on the center of mass. Our objective was to test how leg force control during gait is affected by joint torque variance structure in the amputated limb. Within the framework of the uncontrolled manifold analysis, we measured the Index of Motor Abundance (IMA) to quantify joint torque variance structure of amputated legs and its effect on leg force, where IMA > 0 indicates a stabilizing structure. We further evaluated the extent to which IMA in amputated legs used individual (INV) and coordinated (COV) joint control strategies. Amputated legs produced IMA and INV values similar to intact legs, indicating that torque deviations of the prosthetic ankle can modulate leg force at the end of stance phase. However, we observed much lower COV values in the amputated leg relative to intact legs indicating that biological knee joint torque of the amputated leg does not covary with prosthetic ankle torque. This observation suggests inter-joint coordination during gait is significantly limited as a result of transtibial amputation and may help explain the higher rate of falls and impaired balance recovery in this population, pointing to a greater need to focus on inter-joint coordination within the amputated limb.

Keywords Biomechanics · Locomotion · Amputation · Motor control · Robustness · Uncontrolled manifold

Introduction

Lower limb amputation dramatically alters leg morphology and results in step length, stance duration, joint torque, and leg force asymmetries (Winter and Sienko 1988; Hermodson et al. 1994; Sanderson and Martin 1997; Donker and Beek 2002; Davies and Datta 2003; Nolan et al. 2003; Detrembleur et al. 2005; Su et al. 2007; Kovac et al. 2009; Houdijk et al. 2009; Sagawa et al. 2011; Czerniecki et al. 2012; Svoboda et al. 2012; Bonnet et al. 2014). While these kinematic and kinetic differences have been well described, we lack a complete understanding of how the underlying neuromechanical control of gait may differ for individuals missing important elements of the locomotor system. Lower limb amputation eliminates active control in at least one joint and extinguishes a wealth of sensory information, which limits motor abundance and likely affects lower limb motor control. Individuals with amputations are also more prone to falls (Miller et al. 2001b, a; Curtze et al. 2010, 2012), possibly because they are unable to respond to perturbations as robustly as able-bodied individuals (Nederhand et al. 2012; Wurdeman et al. 2013). Differences in locomotor control could explain the increased fall rate of individuals with amputation because it may illuminate differences in limb control and response to small step-to-step variations. Individuals with unilateral, transtibial amputation also can serve as a model for understanding the role of the ankle–foot complex in human walking. Insights from studying individuals with amputation can provide information about how the neuromuscular system responds to morphological constraint or injury (e.g. in response to orthosis wear, traumatic

Communicated by Francesco Lacquaniti.

✉ Young-Hui Chang
yh.chang@ap.gatech.edu

[1] Exponent, Inc, Farmington Hills, MI, USA

[2] Comparative Neuromechanics Laboratory, School of Biological Sciences, Georgia Institute of Technology, 555 14th St NW, Atlanta, GA 30332-0356, USA

Published online: 21 November 2022

ankle injury, etc.), ultimately providing more information to improve prosthetic and orthotic exoskeleton design and enhance rehabilitation practices.

This work continues our investigations probing the role of ankle and knee coordination in human walking. Previously, we examined the functional contribution of joint torque coordination to maintaining consistent leg power generation in able-bodied walkers (Toney and Chang 2016). Here we refer to leg force as the force generated on the ground by a single leg, which can be measured as the resultant ground reaction force. Leg power refers to the external mechanical power generated by a single leg and acting on the body center of mass. We found that variable ankle torque timing drives the step-to-step leg force adjustments that maintain consistent peak leg power, while simultaneous ankle–knee coupling provided an additional level of control to regulate how these ankle torque deviations were translated up the leg to affect center of mass dynamics. Variable ankle torque timing was achieved with mostly passive structures. Controlled timing of Achilles tendon recoil initiation may act as a physiological motor to amplify power output. Coupled knee torques enabled robust leg-level function by acting as a physiological brake that refined and balanced the effect of ankle torque timing variability on leg force application and leg power output. Controlled ankle torque timing and ankle–knee covariation therefore appear important for robust control of propulsive leg power production in able-bodied walking. In this study, we aim to determine the effect of essentially eliminating active sensorimotor ankle control and ankle–knee neuromechanical coupling while maintaining passive ankle function by studying the motor control of walkers with a transtibial amputation. This approach allows us to gain insight into the role of ankle control and ankle–knee coupling in whole leg function; and, how step-to-step leg force control in walking is achieved differently in amputated legs when compared to non-amputated legs.

We can test how joint torques combine to modulate leg force by applying an uncontrolled manifold (UCM) analysis to periodic walking behavior. The UCM analysis partitions elemental variance into two orthogonal components that contribute to either task stabilization or task modulation (Scholz and Schöner 1999). By comparing the relative amounts of each component, we can determine how elemental variables coordinate to affect the hypothesized task variable. The UCM analysis is based on the principle of motor abundance, meaning that human walkers have more degrees of freedom than necessary to control identified task variables (Bernstein 1967; Scholz and Schöner 1999; Latash 2012). Here, we investigated differences in how individuals with a unilateral transtibial amputation would adjust available degrees of freedom of their biological and prosthetic joint torques within the amputated leg to control this leg force modulation.

Individuals with a transtibial amputation functionally lack the principal muscle group (triceps surae) that controls ankle torque generation. Many individuals with transtibial amputation instead rely on elastic storage and return (ESAR) prosthetic devices that have less precise control and produce less power than biological ankles (Winter and Sienko 1988; Hermodson et al. 1994; Sanderson and Martin 1997; Zmitrewicz et al. 2006; Su et al. 2007; Kovac et al. 2009; Ventura et al. 2011). Compensation for motor control deficiencies on their amputated side are likely accomplished using either the contralateral sound limb, or more proximal joints of the affected limb (Vrieling et al. 2007; Houdijk et al. 2009; Gates et al. 2012a, b; Curtze et al. 2012). However, deafferentation and lack of proprioception is known to inhibit inter-joint coordination in upper extremity reaching (Ghez and Sainburg 1995; Sainburg et al. 1995), suggesting individuals with a lower limb amputation may have similar challenges. Despite obvious differences in magnitude, we expected subjects with an amputation to generate consistent peak leg power at the end of stance phase in both their sound and prosthetic limbs (**H1**), as we have previously observed in control subjects (Toney and Chang 2016). We expected that amputated legs would modulate the trailing limb's leg force to achieve this consistent power output, but hypothesized they would demonstrate less joint torque covariation across their biological and prosthetic joints to achieve these forces than either their contra-lateral sound leg or the legs of able-bodied controls (**H2**).

Methods

Subject characteristics

Eight subjects with a unilateral transtibial amputation (6 M/2F, mass: 80.4 ± 16.9 kg, amputated leg length: 92.2 ± 6.6 cm, sound leg length: 92.0 ± 6.4 cm) and eight healthy, gender-, mass- and leg-length-matched control subjects (6 M/2F, mass: 81.5 ± 14.1 kg, leg length: 91.8 ± 4.7 cm) gave informed consent as approved by the Georgia Institute of Technology Institutional Review Board. Data collected from control subjects were previously reported (Toney and Chang 2016) and are presented here again for ease of comparison. Subjects with an amputation were community ambulators (K3 and K4), able to walk for at least 15 min continuously without assistance or an additional walking aid; wore their own custom-made, well-fitting prosthesis; had an amputation due to trauma or congenital deformity; and had no other known cardiovascular or neurological pathologies. Average time from amputation was 11.9 ± 9.5 years with a range of 1 to 25 years since amputation. Subjects had an average 3.0 ± 1.4 years of experience with the prosthesis worn during testing and reported wearing

their prosthesis an average of 15.4 ± 2.6 h per day. Six of the eight subjects with amputation reported weekly exercise routines including running, cycling, and resistance training. All subjects with an amputation wore their own prosthetic feet while participating in our study. Subjects with an amputation using SACH feet and/or powered ankles were specifically excluded from this study in order to ensure a group of subjects with an amputation who have as similar ankle function to control subjects as possible without the uncertainty of an externally powered device.

Data collection

Four subjects with an amputation completed a 6-min walk test prior to data collection (distance walked: 519.3 m ± 70.3 m, ATS Statement: Guidelines for the 6-min Walk Test). Four of the control subjects completed the 6-min walk test of the same day as data collection, three completed the test on a separate day during a return visit, and one did not complete the test (distance walked: 660.2 ± 56.0 m). All subjects were familiar with treadmill walking. Preferred walking speed was determined by allowing subjects to walk on a custom-built, side-by-side, dual-belt instrumented treadmill at a variety of speeds, first decreasing then increasing from their average speed determined from the 6-min walk test, during which participants verbally indicated whether they would prefer the speed to be faster, slower, or if it was "just right." Subjects who did not complete the 6-min walk test before data collection began walking at a typically comfortable walking speed, 1.3 m/s, when determining their preferred walking speed. All participants walked for 2 min at 75% of their preferred walking speed.

Ground reaction forces were collected independently for each limb as subjects walked on the dual-belt instrumented treadmill (Kram et al. 1998) with embedded force platforms (1080 Hz, Advanced Mechanical Technology Incorporated, Watertown, MA, USA). Simultaneous kinematics data were captured using a six-camera motion analysis system (120 Hz, VICON Motion Systems, Oxford, UK). Retroreflective markers were placed bilaterally on the anterior superior iliac spine, posterior superior iliac spine, greater trochanter, thigh segment, knee joint center, shank segment, lateral malleolus, fifth metatarsal head on the lateral aspect of the foot, and second metatarsophalangeal joint on the foot dorsum. Identical marker sets were used for subjects with an amputation and able-bodied subjects. Prosthetic leg foot and ankle markers were placed as closely matched to the sound leg as possible.

Data analysis

Marker and force data were filtered with a zero-phase lag fourth-order Butterworth low-pass filter with a 10 Hz cut-off frequency. Joint torques were calculated in the sagittal plane using standard inverse dynamics calculations and estimated segment inertial characteristics based on subject specific anthropometrics (Winter 1980). Inertial characteristics of the amputated leg and the prosthetic device were determined with the same method used for intact limbs. Possible errors introduced by using cadaveric rather than measured segmental inertial properties for the amputated leg and prosthetic components likely has little effect on the calculated joint torques during the stance phase of gait (Miller 1987; Winter and Sienko 1988; Powers et al. 1998; Su et al. 2007; Goldberg et al. 2008; Nguyen and Reynolds 2014), which was the focus of our study.

Individual leg power trajectories

Individual leg power is the external mechanical power from the limb of interest acting on the body center of mass and was calculated in the same way for all leg types (control, sound, and amputated). Leg power was calculated as the dot product of the resultant ground reaction force and the body center of mass (COM) velocity (Eq. 1, Donelan et al. 2002a, b). The COM velocity was calculated as the integration of COM acceleration as calculated from the subject mass and the net ground reaction force recorded from both legs (2). The integration constants used were zero for the vertical and medio-lateral components of COM velocity and the set treadmill speed for the anterior–posterior COM velocity component. To compare across subjects, leg power was normalized by body weight and walking speed of each individual.

$$P = F_{\text{leg}} \cdot v_{\text{com}} \tag{1}$$

$$v_{\text{com}} = \int a_{\text{com}} \mathrm{d}t = \int \frac{F_{\text{net}}}{m} \mathrm{d}t \tag{2}$$

Uncontrolled manifold (UCM) analysis

An uncontrolled manifold (UCM) analysis was performed using custom Matlab code. Specific details of this approach have been discussed previously (Yen et al. 2009; Yen and Chang 2010; Toney and Chang 2013, 2016). For clarity, the general approach is outlined here and the differences in how the analysis was applied to the amputated legs are discussed in detail.

To apply the UCM analysis, we must first establish a mathematical relationship relating elemental variables to the task variable. This mathematical relationship defines a task specific Jacobian matrix ($\boldsymbol{J}$) quantifying the effects of small changes in the elemental variables on the hypothesized task variable. The null space of $\boldsymbol{J}$ is therefore a linearized

approximation of the task equivalent manifold, which contains all combinations of elemental variables that yield the same task variable. The measured elemental variance can then be projected onto a two-dimensional space: one dimension parallel to the manifold, containing all elemental variance that has no effect on the task variable (goal equivalent variance, Eq. 3) and one dimension that is orthogonal to the manifold, containing all elemental variance that cause divergence from the task variable (non-goal equivalent variance, Eq. 4), where $\boldsymbol{C}$ is the statistically derived covariance matrix for the elemental variables, $\boldsymbol{n}$ is the number of local degrees of freedom (i.e. number of elemental variables), and $\boldsymbol{d}$ is the number of global degrees of freedom (i.e. number of task variables). The difference between these two components, normalized by the total elemental variance (*TotV*, Eq. 6), is called the index of motor abundance (*IMA*, Eq. 5) and characterizes how the structure of elemental variance affects task-level variance (Auyang et al. 2009; Yen et al. 2009; Yen and Chang 2010; Toney and Chang 2013). An IMA of zero indicates a randomly distributed variance structure. Positive IMA values indicate that more of the elemental variance is goal-equivalent, and the elemental variables non-randomly combine to make the task variable more consistent with each step cycle. Negative IMA values indicate that more of the elemental variance is non-goal equivalent, and the elemental variables tend to combine to modulate the task variable from step-to-step. In this way the UCM analysis provides a window into how the nervous system regulates motor abundance toward a particular functional outcome.

$$\mathrm{GEV} = \frac{\mathrm{trace}\left(\mathrm{null}(J)^T \cdot C \cdot \mathrm{null}(J)\right)}{n-d} \tag{3}$$

$$\mathrm{NGEV} = \frac{\mathrm{trace}\left(\left(J \cdot J^T\right)^{-1} \cdot J \cdot C \cdot J^T\right)}{d} \tag{4}$$

$$\mathrm{IMA} = \frac{(\mathrm{GEV} - \mathrm{NGEV})}{\mathrm{TotV}} \tag{5}$$

$$\mathrm{TotV} = \frac{\mathrm{trace}(C)}{n} \tag{6}$$

We used a dynamically consistent generalized inverse of the kinematic Jacobian relating joint angles to end point position to derive a Jacobian matrix ($\boldsymbol{J}$) that can relate joint torques to the resultant ground reaction force applied to the ground, which we refer to as leg force (Khatib 1987; Yen et al. 2009; Toney and Chang 2013). We used the same Jacobian to relate joint torques to force in the amputated leg as in the able-bodied and sound legs. In doing this, we assume that the prosthetic ankle is a meaningful degree of freedom in determining the leg force. While it cannot be directly actuated by muscle, controlling the way the prosthetic device is loaded and deflected during single support phase of walking can indirectly modify prosthetic ankle torque output. For this reason, we chose to include the prosthetic ankle in the Jacobian and resulting UCM analysis as a first step to understanding how all contributing degrees of freedom influence leg force output.

Components of covariation and individual joint torque control contributing to leg force control

Joint torque variance structure can arise from two possible sources: (i) individual joint torque control and/or (ii) covariance across joints. We previously developed a method for isolating the effects of these two variance sources by manipulating the covariance matrix used to calculate GEV and NGEV (Yen and Chang 2010). The diagonal components of the covariance matrix ($\sigma_a^2, \sigma_k^2, \sigma_h^2$, Eq. 7, where a = ankle, k = knee, and h = hip) contain the variance of each joint relative to itself (individual variance), while the off-diagonal elements describe inter-joint covariance, where a = ankle, k = knee, and h = hip). We can isolate the effect of individual joint torque variance on overall variance structure by setting the off-diagonal covariance components of the covariance matrix (C) to zero (C', Eq. 8) then re-calculating GEV', NGEV', and IMA' using C'. The resulting IMA' indicates the influence of individual joint torque control on leg force output with all influence of joint covariation removed, and we call this new metric INV. All remaining variance structure is due to covariance between the joints, so we can calculate the contribution of inter-joint covariation (COV) to leg force output by subtracting INV from the original IMA (Eq. 9).

$$C = \begin{bmatrix} \sigma_a^2 & \sigma_{ka} & \sigma_{ha} \\ \sigma_{ak} & \sigma_k^2 & \sigma_{hk} \\ \sigma_{ah} & \sigma_{kh} & \sigma_h^2 \end{bmatrix} \tag{7}$$

$$C' = \begin{bmatrix} \sigma_a^2 & 0 & 0 \\ 0 & \sigma_k^2 & 0 \\ 0 & 0 & \sigma_h^2 \end{bmatrix} \tag{8}$$

$$COV = IMA - INV \tag{9}$$

Ankle–knee statistical covariation

The contribution of each joint's individual control and/or coordination between two specific joints (e.g. ankle–knee covariance, σ_{ak}) can be determined from the individual components of the covariance matrix ($\boldsymbol{C}$, Eq. 7). It is important to note that these values of statistical covariance are different

than the abundance metric COV (Eq. 9). The covariance described here is the canonical statistically derived reliance of one joint on another's action, while COV is a metric calculated from our UCM analysis that indicates how much leg force control arises from this source of inter-joint covariation.

Statistical analysis

All statistical test were conducted in SPSS software (IBM, Armonk, NY). We used a 2-sided, paired t test ($\alpha = 0.05$) to test for differences in body mass between the two subject groups. We ran a separate one-way repeated measures ANOVA to test for differences in leg length, magnitude of peak power, and timing of different events, respectively. When the assumption of sphericity was not met, a Greenhouse–Geisser correction was used. We used a 3×1 rmANOVA with leg type as the independent variable to test for leg length differences across the amputated, sound, and matched control leg. We also ran a 3×1 rmANOVA to test for differences in peak leg power magnitude across the same three leg types. To test for differences in the times of peak leg power, minimum IMA, and minimum INV, we ran a 3×1 rmANOVA with time as the independent variable, which was run separately for the sound and amputated legs.

Mean IMA trajectories across all subjects from both groups were evaluated for significant differences from zero using a two-tailed Student's t test ($\alpha = 0.005$, with a Bonferroni correction for 100 comparisons). An IMA significantly greater than zero indicates the local elemental variables (joint-torques) were coordinated to generate the same leg force trajectory, which we interpret as stabilization of a controlled implicit neuromechanical goal of walking. In other words, a positive IMA indicates that task-irrelevant deviations were greater than task-relevant deviations, which is consistent with a minimum intervention principle of motor control (Todorov and Jordan 2002). An IMA significantly less than zero indicates active modulation such that the local variables combined to alter and produce a different leg force trajectory with each successive step. These negative IMA values indicate that task-relevant deviations are not restricted, but instead contribute directly to net-force modulation on each step cycle. A negative IMA is, therefore, interpreted to mean that leg force is not an implicit gait goal, but is instead likely modulated to stabilize some other parameter.

We evaluated the contribution of coordinated and individual joint torque control strategies to leg force control by testing the similarity of the COV and INV trajectories to the IMA trajectory. Testing the similarity of trajectories was accomplished by "fitting" each trajectory to the other using the Matlab function "corrcoef." The resulting R^2 value indicates the amount of inter-subject IMA variance that the COV or INV trajectory is able to explain (Bauman and Chang 2013). In other words, larger R^2 values indicate a better matching of the two trajectories and a greater amount of inter-subject IMA variance can be explained by that particular source of elemental organization (i.e., COV or INV).

Results

Subject characteristics

Matched control subjects did not differ significantly from subjects with an amputation in regards to weight ($p = 0.50$) or leg length ($p = 0.54$), but subjects with an amputation demonstrated a significantly lower preferred walking speed than control subjects (CON: 1.29 ± 0.10 m/s; AMP: 1.17 ± 0.09 m/s; $p < 0.05$) (Table 1).

Joint torques and ground reaction forces

Individual joint torque and resultant ground reaction force trajectories for the sound leg (Fig. 1) and amputated leg (Fig. 2) are consistent with previous published data for subjects with an amputation (Winter and Sienko 1988; Hermodson et al. 1994; Kovac et al. 2009; Sagawa et al. 2011).

Leg power

Individual leg power profiles were similar to previously published data (Donelan et al. 2002a, b). Peak leg power was consistently generated for each leg type (control, sound, and amputated), but amputated legs generated smaller peak power magnitudes than either the sound or control legs.

Table 1 Subject characteristics

	Control legs ($n = 8$)	Sound legs ($n = 8$)	Prosthetic legs ($n = 8$)
Leg length (cm)	91.5 ± 4.9	92.0 ± 6.4	92.2 ± 6.6
Mass (kg)	81.5 ± 14.1	80.4 ± 16.9	
Gender	6 M/2F	6 M/2F	
Preferred walking speed (m/s)	1.29 ± 0.10	1.17 ± 0.09*	

*Significant difference, paired t test, $p < 0.05$

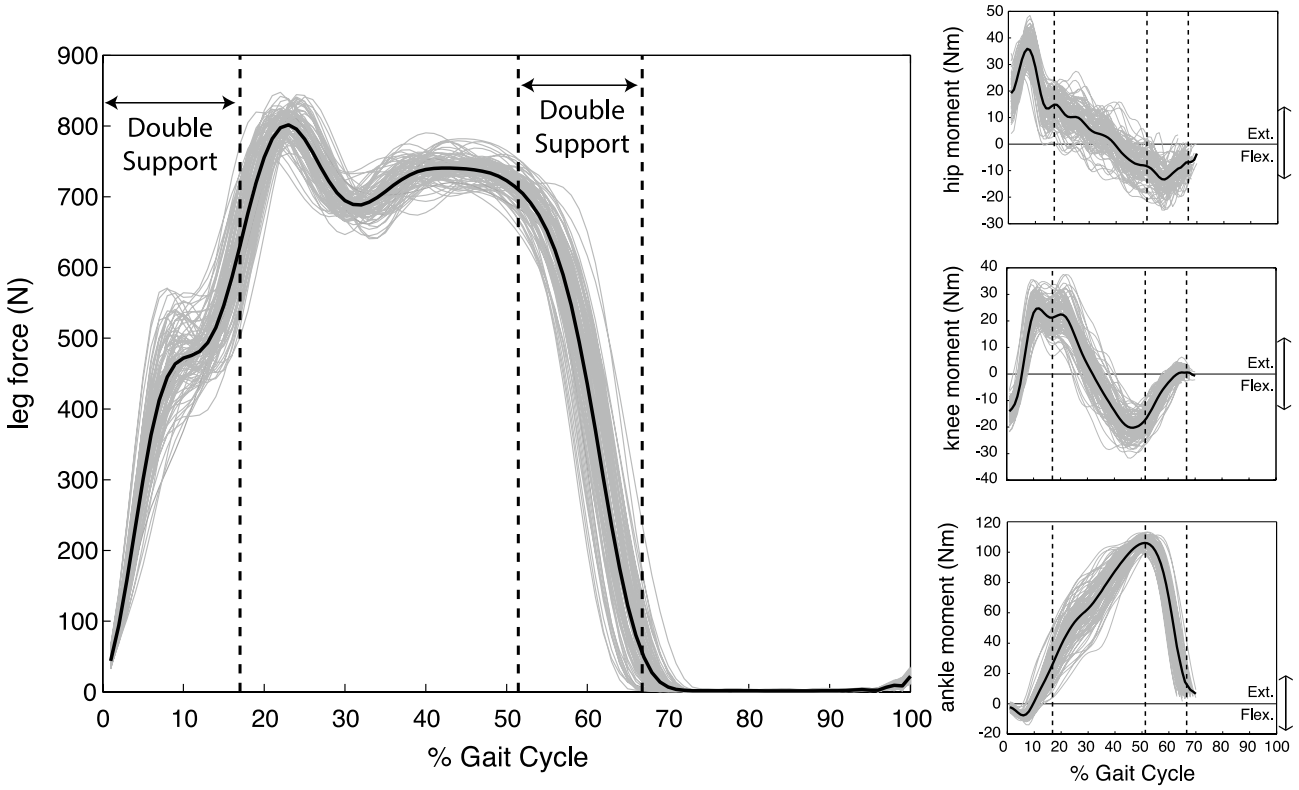

Fig. 1 Representative subject sound leg force as measured by the resultant ground reaction force (left panel) and corresponding joint torques (right column). Gray lines represent leg force and joint torque values for each individual step, while the thick black lines represent the mean trajectory. Double support when the sound leg is leading (1–17.5 ± 1.3% gait cycle) and when the leg is trailing (50.8 ± 3.0–66.8 ± 1.6% gait cycle) are bounded by the dashed vertical lines. Gait cycles are defined from heel contact (0%) to ipsilateral heel contact following swing phase (100%)

Paired times of the peak leg power and of a local minimum in leg power variance were coincident for each respective leg in control (Fig. 3A), sound (Fig. 3B), and amputated legs (Fig. 3C). Control legs generated peak power at 58.5 ± 1.2% of the gait cycle and a local variance minimum at 58.4 ± 1.1% of the gait cycle, which were not significantly different in their timing (paired *t* test, $p = 0.35$). In the sound limb of subjects with an amputation, peak power (60.0 ± 1.3% gait cycle) occurred slightly later than the local variance minimum (59.3 ± 0.9% gait cycle, $p = 0.02$). However, the average timing difference was 0.8 ± 0.7% of the gait cycle, which equates to less than 10 ms, a timing difference likely indistinguishable by the human nervous system. The amputated legs did not have a difference in timing ($p > 0.05$) between peak power (58.8 ± 1.7% gait cycle) and the local variance minimum (58.8 ± 1.7% gait cycle). A repeated measures ANOVA analysis of peak power magnitudes revealed a significant main effect of leg type ($F = 12.614$, $p = 0.001$). The magnitudes of peak power in the prosthetic legs (0.12 ± 0.3% BW*walking speed) were significantly smaller than peak powers in either the sound (0.16 ± 0.04% BW*walking speed; $p = 0.0124$), or the control legs (0.19 ± 0.02% BW*speed; $p = 0.002$). The sound and control leg peak power magnitudes were not significantly different ($p = 0.189$).

Inter-joint model for leg force control

We used a 3-DOF model to test whether each leg's generated force on the ground was stabilized by the inter-joint torque variance structure. Amputated legs demonstrated similar Index of Motor Abundance (IMA) as sound and control legs at specific parts of the gait cycle. IMA values were significantly greater than zero (IMA > 0, $p < 0.005$) for all leg types (Control 1–15% gait cycle; Sound 1–6% and 9% gait cycle; Amputated 1–9% gait cycle) when the leg of interest was leading (Fig. 4A, C, E). Control legs demonstrated IMA values significantly less than zero (IMA < 0, $p < 0.005$) once during single leg stance (44% gait cycle) and during double support when the leg trailed (59–61% gait cycle, Fig. 4A). The sound limbs of subjects with an amputation demonstrated IMA values significantly less than zero (IMA < 0, $p < 0.005$) during the second double support period when the sound leg was trailing (58–64% gait cycle, Fig. 4C). Similar

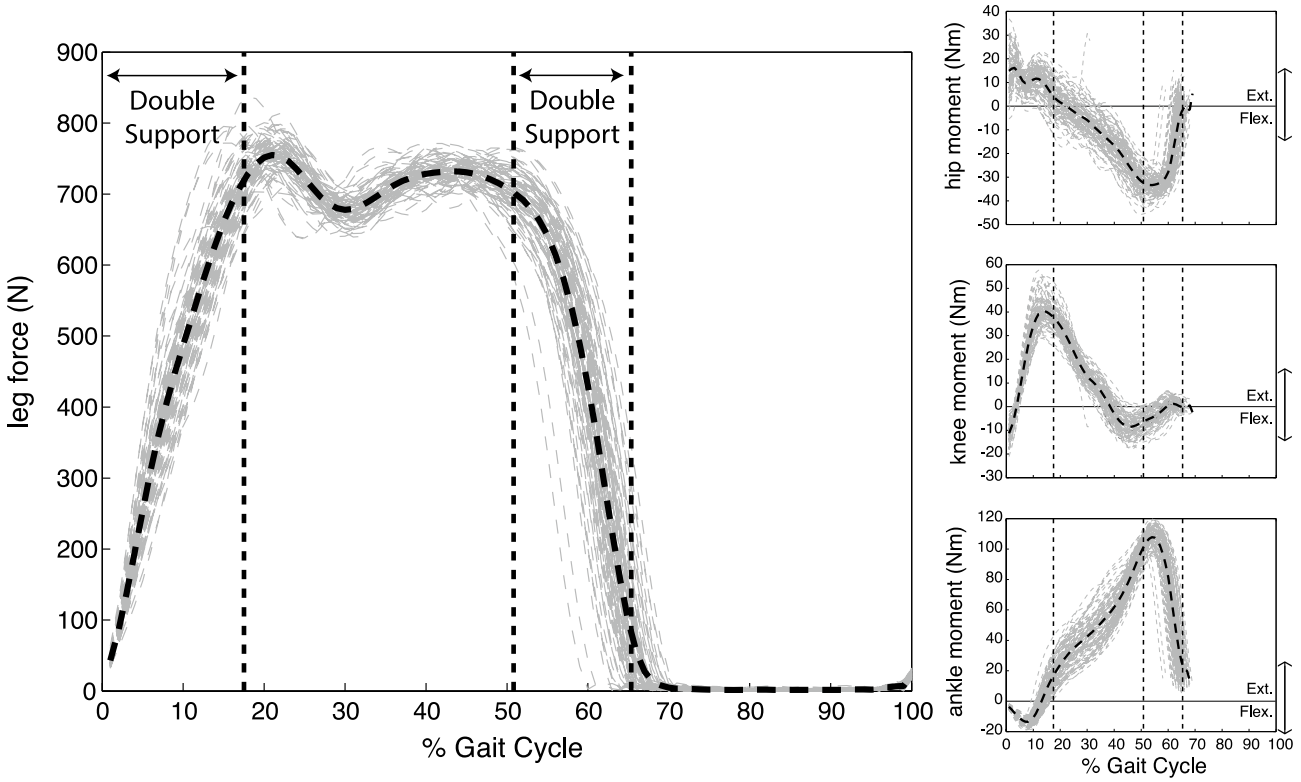

Fig. 2 Representative subject amputated leg force as measured by the resultant ground reaction force (left panel) and corresponding joint torques (right column). Convention is same as for Fig. 1. Gray dashed lines represent leg force and joint torque values for each individual step, while the thick black dashed lines represent the mean trajectory. Double support when the amputated leg is leading (1–17.0 ± 1.1% gait cycle) and when the leg is trailing (51.5 ± 1.3–65.4 ± 1.8% gait cycle) are bounded by the dashed vertical lines. Gait cycles are defined from heel contact (0%) to ipsilateral heel contact following swing phase (100%)

to control and sound limbs, amputated legs demonstrated IMA values significantly less than zero ($p < 0.005$) during double support when the amputated leg trailed and was generating positive power (57–59% gait cycle, Fig. 4E). All leg types (control, sound, and amputated) demonstrated negative IMA values at the same instant they generated peak leg power (Fig. 4, black vertical arrows).

Contribution of individual and coordinated variance structures on leg force control.

Both individual (INV, red line) and coordinated (COV, green line) joint torque control contributed to leg force generation in the sound and amputated legs of subjects with an amputation, but over shorter periods of the gait cycle when compared to able-bodied subjects. Control subject leg forces were influenced by using both individual (INV, red line) and coordinated (COV, green line) joint torque strategies (Fig. 4B). For control subject legs, INV was significantly greater than zero ($INV > 0$, $p < 0.005$) when the leg lead in double support (1–6% gait cycle), and was significantly less than zero ($INV < 0$, $p < 0.005$) for 27% of the total gait cycle during both single limb stance and the second double support period when the leg trailed (26–45% and 57–63% gait cycle). Notably, the time of minimum INV occurred at the same time as peak power generation (Toney and Chang 2016, Fig. 4B, black arrow). In contrast, the COV component of joint torque variance organization was significantly greater than zero for 46% of the gait cycle ($COV > 0$, $p < 0.005$, 9–12%, 14–41%, 51–64% gait cycle), acting to stabilize leg force control throughout the majority of stance phase. The sound leg of subjects with an amputation also demonstrated significant contributions of INV and COV at different points in the gait cycle (Fig. 4D). INV values were significantly greater than zero ($INV > 0$, $p < 0.005$) when the sound leg lead in the first double support period (1–6% gait cycle), and was significantly less than zero ($INV < 0$, $p < 0.005$) for 21% of the gait cycle during single limb stance (24–37% gait cycle) and the second double support period (58–64% gait cycle). The COV component of variance structure was significantly greater than zero ($COV > 0$, $p < 0.005$) for 15% of the total gait cycle, generating a stabilizing effect on leg force for less total time but at similar instances in the gait cycle as control legs when the leg lead in double support (9% gait cycle), single limb stance (32–40% and 50% gait cycle), and when the leg trailed in double support

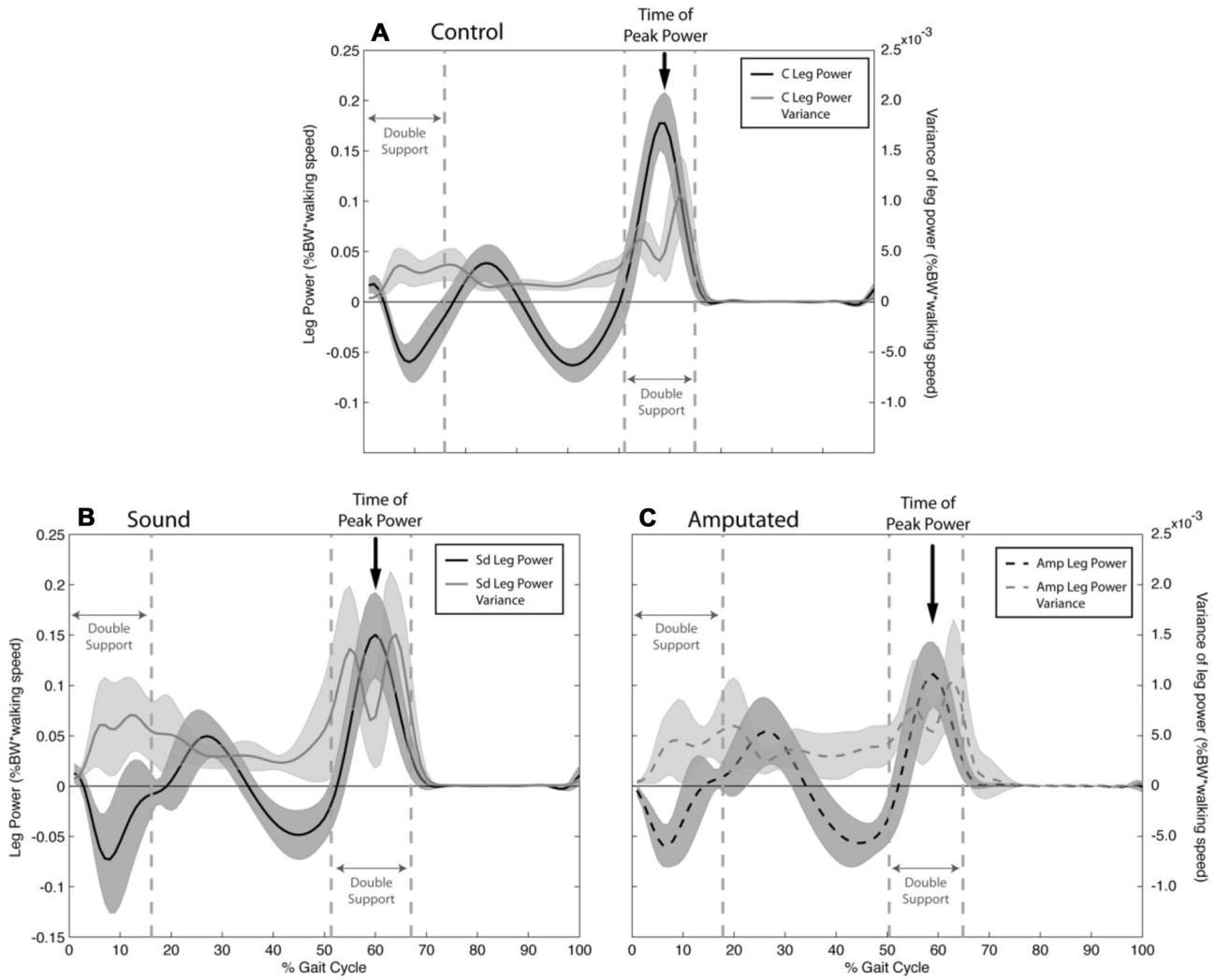

Fig. 3 Mean and standard deviation of leg power as measured by external mechanical power acting on the center of mass (black lines) and variance of leg power (grey lines) for the control (**A**), sound (**B**), and amputated (**C**) legs tested. Peak amputated leg power ($0.12 \pm 0.3\%$ BW*speed) is slightly smaller than the sound leg (0.16 ± 0.04) peak propulsive power (paired t test, $t = 2.4934$, $p = 0.0207$, one-tailed alpha = 0.05). However, both legs demonstrate local minima of leg power variance when leg power is maximal (large vertical arrow), indicating that peak leg power is consistently generated from one step to the next

(60–63% gait cycle). The most negative INV (and IMA) value occurred at the same time as peak leg power in sound limb of subjects with an amputation (rmANOVA, $p = 0.393$, paired t-test (INV&P), $p = 0.5490$), similarly to what was observed in the control legs. Similar to control and sound legs, amputated legs demonstrated INV values significantly greater than zero (INV > 0, $p < 0.005$) when the leg lead in double support (2–7% gait cycle). However, amputated legs demonstrated much shorter periods of negative INV and positive COV contributions to leg force control throughout the gait cycle (Fig. 4F). INV values were significantly less than zero (INV < 0, $p < 0.005$) for only 4% of the gait cycle when the amputated leg trailed in double support (57–60% gait cycle), while COV was significantly greater than zero (COV > 0, $p < 0.005$) for only 3% of the entire gait cycle just before amputated leg toe off (62–64% gait cycle). Like control and sound legs, there was no significant difference in the timing of the most negative INV (and IMA) values from the instant of peak power production (rmANOVA, $F = 0.529$, $p = 0.513$).

Similar to observations in control subjects (Toney and Chang 2016), simple regression analysis showed that INV contributed to the shape of the IMA trajectory more than COV in both sound and amputated legs. Sound leg INV accounted for 97% of the inter-subject residual variance in the sound leg IMA trajectories ($R^2 = 0.97$), while COV only accounted for 26% of residual IMA variance in sound legs ($R^2 = 0.26$). Amputated leg INV accounted for 91% of inter-subject IMA residual variance ($R^2 = 0.91$), but COV only

accounted for 20% of the residual inter-subject variance in the IMA trajectories ($R^2 = 0.20$).

Inter-joint torque covariance

Amputated legs demonstrated less ankle–knee statistical covariance than able-bodied, control subjects throughout the gait cycle. Components of the statistical covariance matrix (C, Eq. 7) revealed ankle and knee joint covariance was significantly greater than zero ($p < 0.005$) in control legs (Fig. 5, solid line) periodically throughout the gait cycle. Positive covariance values indicate that the knee tends to generate a flexion torque when the ankle generates an extension torque, reducing transmission of ankle torque deviations up the leg and having a net stabilizing effect on leg force (Toney and Chang 2016). Amputated legs exhibited a similar mean trajectory to controls during push-off, however, they did not demonstrate any statistically significant ankle–knee covariance in this period nor at any other point in the gait cycle (Fig. 5, dashed line).

Discussion

We investigated the underlying motor control of walking with an amputation by using a modified uncontrolled manifold (UCM) analysis to quantify joint torque variance structure as it relates to generating leg forces on the ground. Subjects with amputation were able to vary ankle torque on their prosthetic ankles to modulate changes in leg force as well as biological ankle joints. In contrast, subjects with amputation were unable to coordinate their biological knee joint torque with joint torque variations in the prosthetic ankle as observed in intact legs.

Subjects with an amputation maintain consistent trailing leg peak power

Subjects with an amputation appear able to generate consistent, albeit smaller, peak leg power values similarly to control legs despite lacking direct ankle torque control. Peak leg power occurred at the same time in the gait cycle as a local minimum in leg power variance for each leg type (Fig. 3). These results indicate that, regardless of leg type, leg power was produced more consistently at its peak than at any other surrounding instant in the leg power trajectory. This finding further suggests that peak leg powers were consistently generated during each step.

Subjects with an amputation generate leg forces similarly to able-bodied subjects

In leading limbs, leg forces were stabilized (IMA > 0) during the double support period in all leg types (Fig. 4). Subjects with an amputation structure their joint torque variance in both their sound and amputated legs similarly to control legs when the leg leads, suggesting that the consistency of leg forces generated during weight acceptance are not affected by a lack of direct ankle torque control. When the leg is trailing in double support and generating push off forces, however, leg forces were modulated by the joint torque variance from step-to-step (IMA < 0) in each leg type (Fig. 4). This result shows that, like intact legs, subjects with an amputation modulate their amputated leg forces at the point in the gait cycle when leg power generation was maximal and also highly consistent across cycles. We previously showed that control subjects stabilize trailing leg peak power through modulation of trailing leg force trajectories with each step (Toney and Chang 2016). Individuals with an amputation also appear able to modulate amputated leg force trajectories to stabilize leg power, despite relying on a passive ankle–foot mechanism to generate leg force and power via elastic energy storage and return. Any locomotor control differences resulting from use of a prosthetic ankle–foot device do not appear to affect the consistency of the leg forces generated by our subjects with unilateral, transtibial amputations. It is worth noting that we specifically recruited participants who were very familiar and skilled with walking using their prescribed prosthetic device. The similar leg force control we observe here may result from the considerable experience and training our participants possess. Individuals with more recent amputations might demonstrate notable differences in leg force control, which may later adapt to more closely resemble the control patterns observed here with training and rehabilitation. In fact, if individuals with new amputations are indeed deficient, achieving leg force modulation for consistent leg power generation might be a useful rehabilitation goal to monitor and target as a metric for improvement.

Amputated legs demonstrate fewer periods of structured joint torque variance throughout the gait cycle

While subjects with an amputation can generate leg force trajectories similar to control subjects, how joint torques were combined to generate these leg force trajectories was different in the amputated legs compared to either the contralateral sound or intact control legs. In terms of affecting leg force consistency, individual joint torque variance structure (INV) contributed the most to total joint torque variance structure (IMA) in all leg types, but the proportion

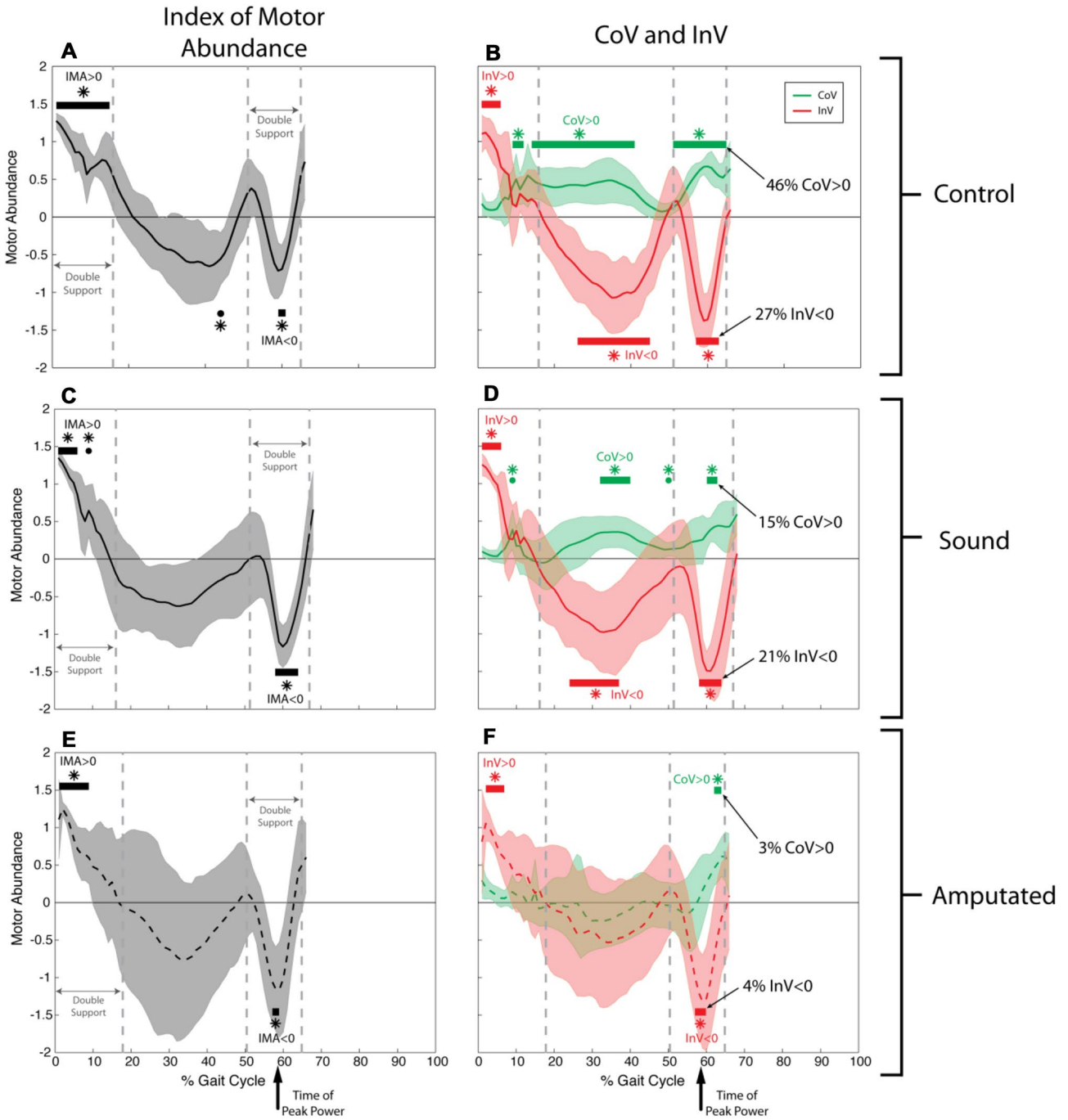

of the gait cycle when INV contributed was smaller in amputated legs as compared to either the sound or control legs (Fig. 4). While the control and sound limbs combined the effects of individual (INV) with coordinated (COV) joint torque control throughout the gait cycle, the amputated legs demonstrated significant contributions from only INV and only over very limited instances within the gait cycle. INV effects were present during weight acceptance and at push off portions of stance phase, when leg forces likely have the most influence on center of mass and whole-body dynamics. Leg mechanics during weight acceptance are largely passive, determined by the preceding step's dynamics and lead leg posture, so the leading leg forces are likely generated as consistently as possible by stabilizing leg orientation and trailing leg power (Kuo et al. 2005; Toney and Chang 2013). Prosthetic ankle torque deviations are, therefore, unlikely to substantially affect leg force output when the leg is leading. During push off in the second double support period, however, ankle torques have the greatest influence on the leg force trajectory (Toney and Chang 2016, Fig. 3). We have

◂**Fig. 4** Joint torque variance structures for control (**A**, **B**), sound (**C**, **D**) and amputated (**E**, **F**) legs throughout the gait cycle. Mean and standard deviation of the Index of Motor Abundance (left column) demonstrates whether joint torques combine to stabilize (IMA > 0) or modulate (IMA < 0) leg force. The components of variance structure (right column) indicate to what degree the ankle, knee, and hip joint torques use a coordination strategy (COV, green) or individual joint control strategy (INV, red) to result in the overall IMA variance structure (IMA = COV + INV). A) Control subjects stabilize leg force (IMA > 0, $p < 0.005$) during double support when the leg is leading (1–15.9 ± 1.4% of gait cycle) and modulate leg force (IMA < 0, $p < 0.005$) from step-to-step when the leg generates maximal power when trailing in double support (51.1 ± 0.8%-64.9 ± 1.1% gait cycle). **B** The individual joint control strategy (INV) has a large influence over IMA values, despite the interjoint coordination strategy acting mainly to stabilize leg force (COV > 0, $p < 0.005$) throughout most of the gait cycle. **C**, **D**) The sound limb of subjects with an amputation behave similarly to those of the control subjects. Leg force stabilization (IMA > 0, $p < 0.005$) when leading in double support (1–16.1 ± 1.3%) and modulation (IMA < 0, $p < 0.005$) when trailing in double support (51.3 ± 1.5%-67.0 ± 1.1%) arise primarily from individual joint torque control (INV). Covariation between joints (COV, green) does not have as persistent an effect in the sound limb of subjects with an amputation as compared to controls. **E** The amputated legs of the subjects with an amputation demonstrate similar overall IMA structure as control and sound limbs. Ankle, knee, and hip joint torques combine to stabilize leg force (IMA > 0, $p < 0.005$) when the leg is leading in double support (1–17.8 ± 1.6%) and modulate leg force (IMA < 0, $p < 0.005$) when the leg is trailing in double support (50.4 ± 1.5%-64.8 ± 1.9%). Subjects with an amputation appear capable of maintaining IMA values similar to intact limbs despite inherent morphological differences. **F** Amputated legs demonstrate similar amounts of individual joint variance structure (INV, red), which contribute to leg force control. However, amputated legs demonstrate no meaningful COV contribution to leg force control. The small amount of COV at the end of stance occurs immediately before liftoff, when leg force is small and has little influence on center of mass mechanics. This pattern may reflect coordination between joint angles to control leg orientation at liftoff, rather than leg force. Overall, subjects with an amputation appear able to control their amputated leg forces similarly to sound limbs through use of only the individual joint control strategy, but are unable to utilize a joint covariation strategy as observed in intact legs

previously postulated that control subjects modulate ankle torque timing by actively altering when Achilles tendon elastic recoil is initiated (Toney and Chang 2016). Individuals with an amputation do not have a functioning Achilles tendon in their amputated leg and must instead rely on elastic recoil from their manufactured passive ankle–foot system to modulate leg forces when the limb is trailing at the end of stance phase. The power generated by ESAR feet is a function of the toe lever deflection (e.g. prosthetic ankle angular displacement) achieved before push off (Ventura et al. 2011). Individuals with lower limb amputations must, therefore, somehow control how their passive device is being loaded and/or unloaded in order to initiate the elastic recoil and modulate ensuing leg forces at the end of stance phase. The specific mechanism walkers with amputations use to regulate passive prosthetic ankle torque remains unclear, but could involve monitoring and correcting of distal socket kinetics (Childers et al. 2014), shank segment inclination angle, included knee joint angle, and/or leg orientation angle. Identifying the specific method of control used by individuals with amputations requires additional investigation. The work presented here demonstrates that prosthetic feet appear able to mimic intact ankle function well with regard to the ability to modulate consistent leg forces over successive steps. This finding supports the idea that although activation of the triceps surae muscle group is required in late stance, ankle joint modulation of leg force in able-bodied, control subjects may be achieved through the active regulation of passive structures such as the Achilles tendon (Ishikawa et al. 2005; Farris and Sawicki 2012; Cronin et al. 2013; Zelik et al. 2014).

While ankle torque modulation may result from a passive mechanism, the effects of ankle torque deviations are mediated through mechanical and/or neural coupling with more proximal joints. Control subjects covary ankle and knee torques (Fig. 5), presumably to adjust the amount of ankle torque deviation translated along the leg to influence center-of-mass whole-body dynamics (Toney and Chang 2013, 2016). Subjects with an amputation lack significant COV throughout the gait cycle on their amputated leg (Fig. 4). Specifically, they lack significant ankle–knee statistical covariance, especially during single support when inter-joint covariation contributes to leg force consistency on their contralateral leg and in control subjects (i.e., COV > 0, Fig. 5). Statistical covariance between the prosthetic ankle and the residual biological knee was also limited compared to control legs. The lack of significant ankle–knee covariance in subjects with an amputation suggests that the knee joint is mechanically and/or neurally coupled to ankle function in able-bodied subjects. Reduced ankle–knee covariance indicates that the biological knee does not respond to passive prosthetic foot–ankle torque deviations in the same way that biological ankle and knee torque deviations covary in control subjects. In other words, prosthetic ankle plantar-flexion torque deviations are not counterbalanced by a knee flexion torque as Toney and Chang (2016) observed in able-bodied subjects. Increasing the magnitude of sensory signals via vibratory stimulation under the prosthetic foot can improve feedforward, open-loop postural responses, suggesting that sensory feedback from distal structures play an important role in movement coordination (Rusaw et al. 2012). Some biarticular ankle plantar-flexor muscles (i.e., gastrocnemius muscle) are mechanically coupled to also cause knee flexion and provide inter-joint stability in intact legs (Nichols 1999). Following a transtibial amputation, however, triceps surae activation is unable to generate ankle plantar-flexion. In this way, the neuro-mechanical ankle–knee joint coupling typical in a biologically intact leg no longer exists. Recent robotic prosthetic and exoskeletal ankle–foot systems have incorporated the concept of an artificial biarticular gastrocnemius

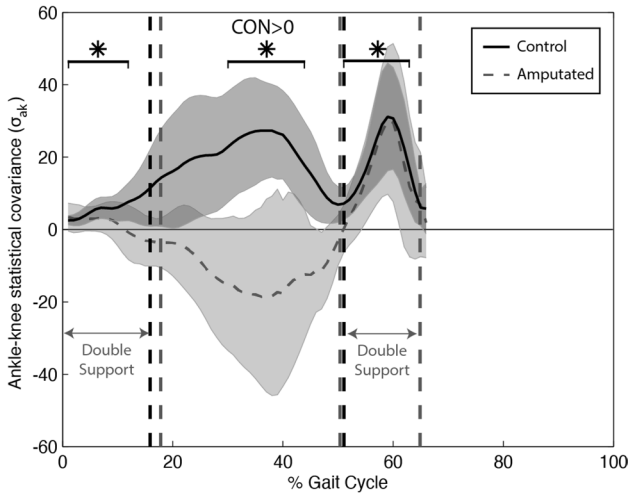

Fig. 5 Mean and standard deviations of statistical covariance (as taken from the covariance matrix, C, from Eq. 7) between ankle and knee torques in control (solid) and amputated (dashed) legs. Control subjects (CON) demonstrate significantly positive ankle–knee covariation ($p < 0.005$) throughout the gait cycle, while the amputated legs of the subjects with an amputation do not demonstrate any significant covariance. *Indicates $p < 0.05$ for the control subjects only

muscle to leverage the importance of ankle–knee coupling (Eilenberg et al. 2018; Malcolm et al. 2018). The energetic benefits of an artificial gastrocnemius were observed in both systems. Malcolm and colleagues also observed a more normal ankle–knee joint coordination when an exoskeleton included an artificial biarticular muscle, however, its effects on leg force control remain unknown. Regardless of the mechanics underlying this deficit, subjects with an amputation do not appear to actively or passively covary knee and ankle torque deviations on their amputated leg. Individuals with amputations are, therefore, less able to appropriately respond to unexpected prosthetic ankle torque deviations with their biological joints resulting in less robust leg force control. This limitation could possibly explain why reduced stability and increased fall risk is observed in walkers with amputations (Miller et al. 2001b, a; Curtze et al. 2010, 2012), however, further investigation is necessary.

A potential limitation of this work is that all subjects walked on a treadmill at their own preferred walking speed. Subjects with an amputation exhibited a small but significant difference of 0.12 m/s in preferred walking speed compared to their matched controls (Table 1), which may have had an unintended effect on measured biomechanical parameters. In a review and meta-analysis on the effect of walking speed on gait biomechanics, Fukuchi et al. (2019), showed significant effects when adults walk at speeds slower or faster than their comfortable range of walking speeds. All subjects from both groups in this study walked within the comfortable range as defined for both young and older adults (2019). Therefore, we expect any differences due to gait speed to have minimal effect on our general conclusions about control strategy. Moreover, studying variance in walking parameters may seem counterintuitive since average walking speed is artificially constrained on a treadmill. However, the use of a treadmill is actually a strength rather than a limitation in this regard as it provided a controlled walking environment to test how joint variance is structured relative to specific limb-level task goals within the framework of the UCM analysis. The UCM analysis relies on the presence of small cycle-to-cycle deviations over many repeated step cycles. Collecting data from a treadmill allowed us to collect numerous step cycles that were similar in trajectory, but still contained enough variability to accurately quantify the joint torque variance structure in relation to the hypothesized task variable leg force. Finally, we limited our study to subjects using an ESAR prosthetic foot, which is a popularly prescribed passive prosthesis for persons with amputation who maintain active lifestyles. It is possible that an actively powered prosthesis or a passive one without dynamic response capability could lead to different results. This area would be important for further study using the current findings as a baseline to understand the locomotor coordination strategies used for hybrid control of biological and prosthetic joints.

Conclusion

In this study, we applied a modified uncontrolled manifold (UCM) analysis to steady-state walking of subjects with a lower limb amputation to test how the locomotor system responds to a morphological constraint. Our results show that, despite loss of ankle sensorimotor function, subjects with an amputation maintain step-to-step consistency in whole-body dynamics and leg power production during steady-state walking. However, joint torque covariation was significantly affected by loss of sensory feedback and active motor control from the lower limb amputation. While subjects with an amputation were able to utilize the passive properties of their prosthetic device to modulate leg force, they do not use covariation between their biological knee and prosthetic ankle as subjects with intact legs do to control force. Metaphorically speaking, this control strategy could be compared to controlling the speed of an automobile with an accelerator, but without brakes to temper any unexpected variability in acceleration. The lack of inter-joint covariation limits robust control of leg force and may help to explain why individuals with amputations are more prone to falls or other detrimental gait-related events. Rehabilitation practices and prosthetic design may benefit from additional attention to coordinated function of the ankle and knee during gait. Training impaired individuals to utilize their inherent motor abundance would also enable more flexible

responses to unexpected perturbations and could aid adaptation and long-term motor learning.

Author contributions All authors contributed to the study conception and design. Material preparation, data collection and analysis were performed by MT-B. The first draft of the manuscript was written by MT-B and all authors commented on previous versions of the manuscript. All authors read and approved the final manuscript.

Funding This work was supported in part by National Institutes of Health Grants NICHD 5T32HD055180, NINDS 5R01NS069655, and National Science Foundation Grant 1734416.

Data availability The datasets generated during and/or analyzed during the current study are available from the corresponding author on reasonable request.

Declarations

Conflict of interest The authors have no financial or proprietary interests in any material discussed in this article.

References

Auyang AG, Yen JT, Chang Y-H (2009) Neuromechanical stabilization of leg length and orientation through interjoint compensation during human hopping. Exp Brain Res 192:253–264. https://doi.org/10.1007/s00221-008-1582-7

Bauman JM, Chang YH (2013) Rules to limp by: Joint compensation conserves limb function after peripheral nerve injury. Biol Lett 9:20130484. https://doi.org/10.1098/rsbl.2013.0484

Bernstein N (1967) The co-ordination and regulation of movements. Pergamon Press, Oxford

Bonnet X, Villa C, Fodé P et al (2014) Mechanical work performed by individual limbs of transfemoral amputees during step-to-step transitions: effect of walking velocity. Proc Inst Mech Eng [h] 228:60–66. https://doi.org/10.1177/0954411913514036

Cronin NJ, Avela J, Finni T, Peltonen J (2013) Differences in contractile behaviour between the soleus and medial gastrocnemius muscles during human walking. J Exp Biol 216:909–914. https://doi.org/10.1242/jeb.078196

Curtze C, Hof AL, Otten B, Postema K (2010) Balance recovery after an evoked forward fall in unilateral transtibial amputees. Gait Posture 32:336–341. https://doi.org/10.1016/j.gaitpost.2010.06.005

Curtze C, Hof AL, Postema K, Otten B (2012) The relative contributions of the prosthetic and sound limb to balance control in unilateral transtibial amputees. Gait Posture 36:276–281. https://doi.org/10.1016/j.gaitpost.2012.03.010

Czerniecki JM, Turner AP, Williams RM et al (2012) Mobility changes in individuals with dysvascular amputation from the presurgical period to 12 months postamputation. Arch Phys Med Rehabil 93:1766–1773. https://doi.org/10.1016/j.apmr.2012.04.011

Davies B, Datta D (2003) Mobility outcome following unilateral lower limb amputation

Detrembleur C, Vanmarsenille JM, de Cuyper F, Dierick F (2005) Relationship between energy cost, gait speed, vertical displacement of centre of body mass and efficiency of pendulum-like mechanism in unilateral amputee gait. Gait Posture 21:333–340. https://doi.org/10.1016/j.gaitpost.2004.04.005

Donelan JM, Kram R, Kuo AD (2002a) Mechanical work for step-to-step transitions is a major determinant of the metabolic cost of human walking. J Exp Biol 205:3717–3727

Donelan JM, Kram R, Kuo AD (2002b) Simultaneous positive and negative external mechanical work in human walking. J Biomech 35:117–124

Donker SF, Beek PJ (2002) Interlimb coordination in prosthetic walking: effects of asymmetry and walking velocity. Acta Psychol (Amst) 110:265–288. https://doi.org/10.1016/S0001-6918(02)00037-9

Eilenberg MF, Kuan JY, Herr H (2018) Development and evaluation of a powered artificial gastrocnemius for transtibial amputee gait. J Robot. https://doi.org/10.1155/2018/5951965

Farris DJ, Sawicki GS (2012) Linking the mechanics and energetics of hopping with elastic ankle exoskeletons. J Appl Physiol 113:1862–1872. https://doi.org/10.1152/japplphysiol.00802.2012

Fukuchi CA, Fukuchi RK, Duarte M (2019) Effects of walking speed on gait biomechanics in healthy participants: a systematic review and meta-analysis. Syst Rev 8:153. https://doi.org/10.1186/s13643-019-1063-z

Gates DH, Darter BJ, Dingwell JB, Wilken JM (2012a) Comparison of walking overground and in a computer assisted rehabilitation environment (CAREN) in individuals with and without transtibial amputation. J Neuroeng Rehabil. https://doi.org/10.1186/1743-0003-9-81

Gates DH, Dingwell JB, Scott SJ et al (2012b) Gait characteristics of individuals with transtibial amputations walking on a destabilizing rock surface. Gait Posture 36:33–39. https://doi.org/10.1016/j.gaitpost.2011.12.019

Ghez C, Sainburg R (1995) Proprioceptive control of interjoint coordination. Can J Physiol Pharmacol 73:273–284. https://doi.org/10.1139/y95-038

Goldberg EJ, Requejo PS, Fowler EG (2008) The effect of direct measurement versus cadaver estimates of anthropometry in the calculation of joint moments during above-knee prosthetic gait in pediatrics. J Biomech 41:695–700. https://doi.org/10.1016/j.jbiomech.2007.10.002

Hermodson Y, Ekdahl C, Persson BM, Roxendal G (1994) Gait in male trans-tibia1 amputees: a comparative study with healthy subjects in relation to walking speed

Houdijk H, Pollmann E, Groenewold M et al (2009) The energy cost for the step-to-step transition in amputee walking. Gait Posture 30:35–40. https://doi.org/10.1016/j.gaitpost.2009.02.009

Ishikawa M, Komi PV, Grey MJ et al (2005) Muscle-tendon interaction and elastic energy usage in human walking. J Appl Physiol 99:603–608. https://doi.org/10.1152/japplphysiol.00189.2005

Khatib O (1987) A unified approach for motion and force control of robot manipulators: the operational space formulation. IEEE J Robot Automat 3:43–53. https://doi.org/10.1109/JRA.1987.1087068

Kovac I, Medved V, Ostojic L (2009) Ground reaction force analysis in traumatic transtibial amputees' gait. Coll Antropol 33:107–114

Kram R, Griffin TM, Maxwell Donelan J, Chang Y-H (1998) Force treadmill for measuring vertical and horizontal ground reaction forces. J Appl Physiol 85:764–769

Kuo AD, Maxwell Donelan J, Ruina A, et al (2005) Energetic consequences of walking like an inverted pendulum: step-to-step transitions

Latash ML (2012) The bliss (not the problem) of motor abundance (not redundancy). Exp Brain Res 217:1–5

Lee Childers W, Prilutsky BI, Gregor RJ (2014) Motor adaptation to prosthetic cycling in people with trans-tibial amputation. J Biomech 47:2306–2313. https://doi.org/10.1016/j.jbiomech.2014.04.037

Malcolm P, Galle S, Derave W, de Clercq D (2018) Bi-articular knee-ankle-foot exoskeleton produces higher metabolic cost reduction than weight-matched mono-articular exoskeleton. Front Neurosci. https://doi.org/10.3389/fnins.2018.00069

Miller DI (1987) Resultant lower extremity joint moments in below-knee amputees during running stance. J Biomech 20:529–541
Miller WC, Deathe AB, Speechley M, Koval J (2001a) The influence of falling, fear of falling, and balance confidence on prosthetic mobility and social activity among individuals with a lower extremity amputation. Arch Phys Med Rehabil 82:1238–1244. https://doi.org/10.1053/apmr.2001.25079
Miller WC, Speechley M, Deathe B (2001b) The prevalence and risk factors of falling and fear of falling among lower extremity amputees. Arch Phys Med Rehabil 82:1031–1037. https://doi.org/10.1053/apmr.2001.24295
Nederhand MJ, van Asseldonk EHF, der Kooij H, van Rietman HS (2012) Dynamic balance control (DBC) in lower leg amputee subjects; contribution of the regulatory activity of the prosthesis side. Clin Biomech 27:40–45. https://doi.org/10.1016/j.clinbiomech.2011.07.008
Nguyen TC, Reynolds KJ (2014) The effect of variability in body segment parameters on joint moment using Monte Carlo simulations. Gait Posture 39:346–353. https://doi.org/10.1016/j.gaitpost.2013.08.002
Nichols TR (1999) Receptor mechanisms underlying heterogenic reflexes among the triceps surae muscles of the cat. J Neurophysiol 81:467–478
Nolan L, Wit A, Dudziñ K et al (2003) Adjustments in gait symmetry with walking speed in trans-femoral and trans-tibial amputees. Gait Posture 17:142–151
Powers CM, Rao S, Perry J (1998) Knee kinetics in trans-tibial amputee gait
Rusaw D, Hagberg K, Nolan L, Ramstrand N (2012) Can vibratory feedback be used to improve postural stability in persons with transtibial limb loss? J Rehabil Res Dev 49:1239–1253. https://doi.org/10.1682/JRRD.2011.05.0088
Sagawa Y, Turcot K, Armand S et al (2011) Biomechanics and physiological parameters during gait in lower-limb amputees: a systematic review. Gait Posture 33:511–526
Sainburg RL, Ghilardi MF, Poizner H, Ghez C (1995) Control of limb dynamics in normal subjects and patients without proprioception
Sanderson DJ, Martin PE (1997) Lower extremity kinematic and kinetic adaptations in unilateral below-knee amputees during walking
Scholz JP, Schöner G (1999) The uncontrolled manifold concept: identifying control variables for a functional task. Exp Brain Res 126:289–306. https://doi.org/10.1007/s002210050738
Su PF, Gard SA, Lipschutz RD, Kuiken TA (2007) Gait characteristics of persons with bilateral transtibial amputations. J Rehabil Res Dev 44:491–501. https://doi.org/10.1682/JRRD.2006.10.0135
Svoboda Z, Janura M, Cabell L, Elfmark M (2012) Variability of kinetic variables during gait in unilateral transtibial amputees. Prosthet Orthot Int 36:225–230. https://doi.org/10.1177/0309364612439572
Todorov E, Jordan MI (2002) Optimal feedback control as a theory of motor coordination. Nat Neurosci 5:1226–1235. https://doi.org/10.1038/nn963
Toney ME, Chang YH (2013) Humans robustly adhere to dynamic walking principles by harnessing motor abundance to control forces. Exp Brain Res 231:433–443. https://doi.org/10.1007/s00221-013-3708-9
Toney ME, Chang YH (2016) The motor and the brake of the trailing leg in human walking: leg force control through ankle modulation and knee covariance. Exp Brain Res 234:3011–3023. https://doi.org/10.1007/s00221-016-4703-8
Ventura JD, Klute GK, Neptune RR (2011) The effect of prosthetic ankle energy storage and return properties on muscle activity in below-knee amputee walking. Gait Posture 33:220–226. https://doi.org/10.1016/j.gaitpost.2010.11.009
Vrieling AH, van Keeken HG, Schoppen T et al (2007) Obstacle crossing in lower limb amputees. Gait Posture 26:587–594. https://doi.org/10.1016/j.gaitpost.2006.12.007
Winter DA (1980) Overall principle of lower limb support during stance phase of gait. J Biomech 13:923–927
Winter DA, Sienko SE (1988) Biomechanics of below-knee amputee gait. J Biomech 21:361–367
Wurdeman SR, Myers SA, Stergiou N (2013) Transtibial amputee joint motion has increased attractor divergence during walking compared to non-amputee gait. Ann Biomed Eng 41:806–813. https://doi.org/10.1007/s10439-012-0705-2
Yen JT, Chang YH (2010) Rate-dependent control strategies stabilize limb forces during human locomotion. J R Soc Interface 7:801–810. https://doi.org/10.1098/rsif.2009.0296
Yen JT, Auyang AG, Chang YH (2009) Joint-level kinetic redundancy is exploited to control limb-level forces during human hopping. Exp Brain Res 196:439–451. https://doi.org/10.1007/s00221-009-1868-4
Zelik KE, Huang TWP, Adamczyk PG, Kuo AD (2014) The role of series ankle elasticity in bipedal walking. J Theor Biol 346:75–85. https://doi.org/10.1016/j.jtbi.2013.12.014
Zmitrewicz RJ, Neptune RR, Walden JG et al (2006) The effect of foot and ankle prosthetic components on braking and propulsive impulses during transtibial amputee gait. Arch Phys Med Rehabil 87:1334–1339. https://doi.org/10.1016/j.apmr.2006.06.013

Publisher's Note Springer Nature remains neutral with regard to jurisdictional claims in published maps and institutional affiliations.

Springer Nature or its licensor (e.g. a society or other partner) holds exclusive rights to this article under a publishing agreement with the author(s) or other rightsholder(s); author self-archiving of the accepted manuscript version of this article is solely governed by the terms of such publishing agreement and applicable law.